Contributed paper

OPTO-ELECTRONICS REVIEW 7(4), 313–320 (1999)

A new type of dielectric bolometer mode of infrared detector using ferroelectric thin film capacitors for uncooled focal plane array

M. NODA[1*], K. HASHIMOTO[2], R. KUBO[3], H. TANAKA[4], T. MUKAIGAWA[5], H. XU[1], and M. OKUYAMA[1]

[1]Area of Materials and Device Physics, Department of Physical Science
Graduate School of Engineering Science, Osaka University, Osaka 560, Japan
[2]Human Environment System Development Center, Matsushita Electric Industrial Co., Ltd.
3-1-1, Yagumo-nakamachi, Moriguchi, Osaka 570-8501, Japan
[3]R&D Division, Murata MFG. Co., Ltd., Kanagawa 226, Japan
[4]Solid State Advance Center, Yamatake-Honeywell Co., Ltd., Kanagawa, 1-12-2 Kawana Fujisawa, 251-8522, Japan
[5]Fundamental Research Section, R&D Laboratories, Hochiki Co., Ltd., 246, Tsuruma Machida, Tokyo 194, Japan

We have developed a new type of detector pixel circuit operated in an infrared image sensor of dielectric bolometer mode. The detector pixel consists of capacitors of ferroelectric thin film, whose dielectric constant changes drastically with temperature. After comparing a few kind of ferroelectric materials such as $Ba_{1-x}Sr_xTiO_3$ (BST) and La modified $Sr_{1-x}Ba_xNb_2O_6$ (SBN) among each other, the BST is selected as the ferroelectric film in the structure of the detector. Our proposed circuit is a serially connected capacitor-capacitor, where one capacitor is composed of a BST ferroelectric thin film irradiated by infrared light and the other is nonirradiated one. BST film has been prepared on Si membrane structure by pulsed laser deposition method (PLD). Dielectric constant of the BST film, which is about 450 at 25°C, changes by about 1 to 10% K^{-1} at ambient temperature. As a result of on-board evaluation of the assembled circuit with a source-follower output, the output level is about 40 mV when a relative capacitance change in the capacitor is about 3%. On the other hand, in PSPICE circuit simulations, the output level is about 25 mV when a relative capacitance change in the capacitor of about 100 pF is 1%. The simulated relationship between the output voltage of the assembled circuit and capacitance change of the BST film agrees well with that in the experimental results. It is considered that the circuit has enough output signal level for input of conventional operational amplifier. Voltage responsivity R_v, and specific detectivity D^* estimated from temperature change of dielectric constant are 50 kVW^{-1} and 6.5×10^9 $cmHz^{1/2}W^{-1}$, respectively, which means high-sensitivity compared to the other type of IR sensors. The pixel structure also shows a simple configuration, and then is very effective in reducing their pixel size and then increasing the pixel density.

Keywords: dielectric bolometer mode, detector pixel, ferroelectric thin film, infrared image sensor, circuit simulation.

1. Introduction

Recently, infrared uncooled focal plane arrays (UFPAs) gather much attention because thermal imaging can be easily realized and has shown a wide market of great potential [1,2]. Quite recently, UFPAs based on resistive bolometer have been developed and are becoming commercially available [3,4]. However, a voltage drop across a detector resistance is detected in the resistive bolometer, and so current consumption at the detector is not negligible. This causes tempera-

*e-mail: mnoda@seis.tri.pref.osaka.jp

ture increase in comparison with the real target temperature and limits detectivity. As another candidate of UFPA, both pyroelectric sensor and dielectric bolometer using ferroelectric material show higher responsivity than that of the resistive bolometer. There have been reported some better results of voltage responsivity (R_v), detectivity (D*), and noise equivalent temperature difference (NETD) for the both types of sensors using ferroelectric material [6,7] compared to those using resistive bolometer [3–5]. And also temperature coefficient of dielectric constant is larger, as will be described below, than that of resistance of around 2% K^{-1} of VO_x [5]. So, these kinds of ferroelectric sensors are expected to be applied for fabrication of high-sensitive UFPAs.

Temperature dependence of either polarization or relative permittivity for ferroelectrics can be used for the thermal sensors using ferroelectric material. The former is referred to the traditional pyroelectric (PE) sensor and the latter is to dielectric bolometer (DB). In PE mode, an IR light chopper is needed inconveniently because pyroelectric current is generated when temperature is changed.

This is disadvantageous to get high-sensitive and compact IR sensors compared to those of the other types. In the DB mode, the dielectric constant change against temperature is detected through the capacitance change in the ferroelectric thin film such as $Ba_{1-x}Sr_xTiO_3$ (barium strontium titanate, BST), $Pb(Mg_{1/3}Nb_{2/3})O_3$-$PbTiO_3$ (PMN-PT), $Pb(Sc,Ta)O_3$ (PST), and $Sr_{1-x}Ba_xNb_2O_6$ (SBN) and the chopper is not needed. In order to establish uncooled infrared image sensor arrays in dielectric bolometer mode based on ferroelectric thin film capacitors with high sensitivity and high resolution, we have been developing thermally isolated structures for detector pixel, BST ferroelectric thin film, and both detector pixel and readout circuits.

This paper deals with:

- the circuit design for dielectric bolometer mode of detector pixel and its simulated results,
- selection of ferroelectric material and preparation of BST ferroelectric thin films by pulsed laser deposition (PLD) and characterization for dielectric bolometer mode capacitor,
- fabrication of thermally isolated membrane structure by Si bulk micromachining process (the supported structure and ferroelectric thin film characteristics were optimized for obtaining a high temperature change in the detector pixel),
- finally, we show the experimental results of the circuit operating in dielectric bolometer mode.

2. Circuit consideration for dielectric bolometer mode of detector pixel

2.1. Circuit design

The circuits have been designed for newly invented dielectric-bolometer pixels. The principle of our proposed circuit is based on an intrinsic characteristic of BST ferroelectric material. A main operation in the dielectric bolometer-type detector is as follows:

- when temperature of ferroelectric material in the detector pixel is increased, its dielectric constant changes and therefore its capacitance becomes changed,
- the change in the capacitance is detected as voltage change, which is amplified through some operational amplifiers.

As for capacitor sensors, several types of basic circuits such as capacitor-capacitor bridge, resistor-capacitor bridge, and those without reference circuit part have been proposed and considered. These basic pixel circuits have been simulated including X-Y addressing switch MOSFET's by using PSPICE [8,9]. Figure 1 shows one example of the detector pixel circuits for simulations; capacitor-capacitor seri-

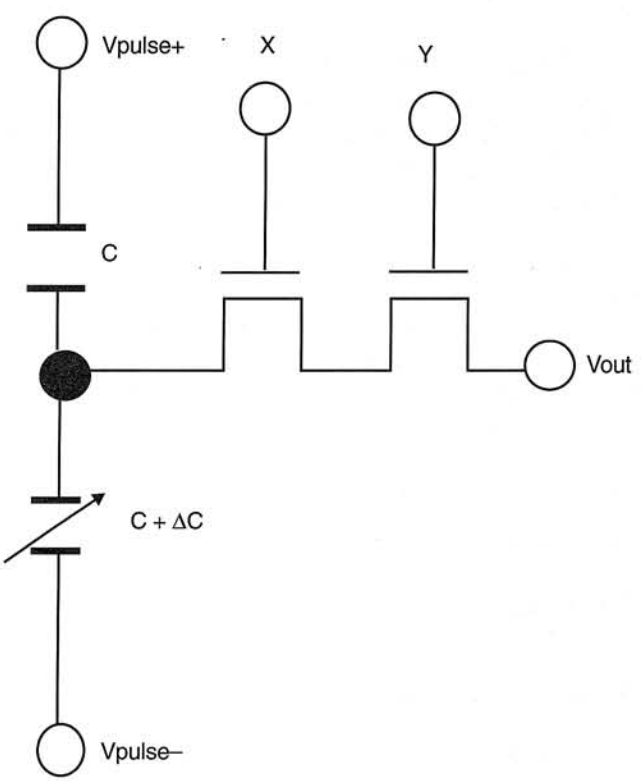

Fig. 1. One example of detector pixel circuits for PSPICE simulations.

ally connected circuit. The proposed circuits have their own merits and demerits in performances such as output voltage, number of components and cell size. The capacitor-capacitor type has been chosen at present stage. Because its output voltage is, in principle, decided by the ratio of the two capacitors even under different ambient temperature, and retention time of the output voltage level becomes very long and is kept nearly constant if leakage current in the capacitor is much small. In other words the steady state output are determined only by the ratio of the capacitances. This eases us to detect a minute change in the voltage level.

Layout patterns have been designed for the above basic pixel circuits and resultant 4×4 UFPAs. Especially the pixel structure shown in Fig. 1 is a simple configuration, and then is very effective in reducing its pixel size and then increasing the pixel density in an UFPA. In our first stage, it is needed to confirm the operation in the basic pixel circuit and the possibility of two-dimensional operations. The ferroelectric capacitor size is about 70 μm to 150 μm square, and the cell size is between about 250 μm to 500 μm square, where our design rules of minimum interconnection are 10 μm line and 15 μm space, respectively.

2.2. Simulation results

Figure 2(a) shows a simple timing chart of pulse supply voltages, Vpulse+ and Vpulse–, gate voltages of X-column switching FET(X) and Y-row switching FET(Y), and output voltages of a specific pixel (X,Y), respectively. The detailed transient response of the output voltage (Vout) waveform in Fig. 2(a) is shown in Fig. 2(b). Its pulse width is 15 μs as explained below.

The MOSFET's in the pixel circuit were fabricated considering the substrate resistance and implantation dose, and their characteristics were evaluated. Major measured results in the FET characteristics have been used for device parameters in PSPICE. The conditions in the simulation are as follows; capacitance in the detecting capacitor was made changed from 100 pF to 101 pF, which means the change ratio is 1%, by increment of 0.2 pF. Transient responses of the simulated output voltages are shown in Fig. 2(b) as a parameter of the change ratio. Two pulse voltage sources, Vpulse+ and Vpulse-, are +5 V and -5 V at ON state, and 0 V at OFF state, respectively, and their ON and OFF times in the pulse period of 200 μs are 100 μs. Gate length and width in the X-Y addressing switch MOSFET's are 10 μm and 10 μm, respectively. And ON time of both (X and Y) switch FET's is 15 μs from the beginning of ON duration times of the pulse voltage source. In the PSPICE simulation, the output waveform is almost square-like shape without a large CR delay because we assume that leakage current parallel to capacitance component is very low in the BST film, although some transient waveform are seen when an equivalent parallel resistance in the BST capacitor is less than 1 MΩ when the corresponding parallel capacitance is around 100 pF.

Figure 3 shows the simulation results of the detector pixel circuit shown in Fig. 1. It is found in the simulation results that when relative capacitance change in the capacitor of 100 pF is 1%, the output voltage

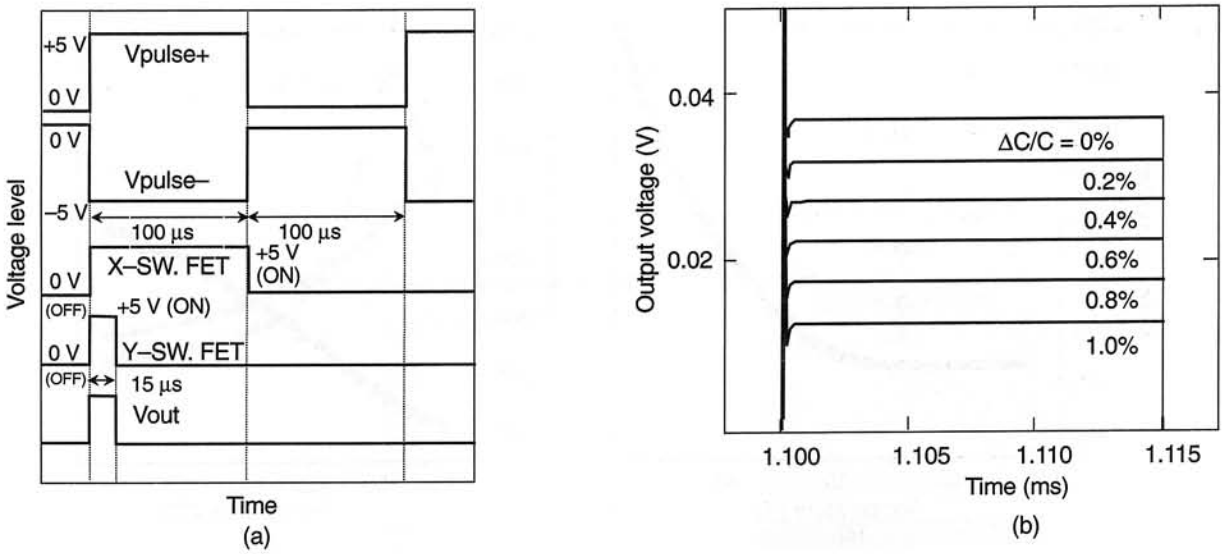

Fig. 2. Simple timing chart of voltages in the detector pixel circuit shown in Fig. 1 (a), and simulated output transient of the detector pixel circuit with different ΔC/C (b).

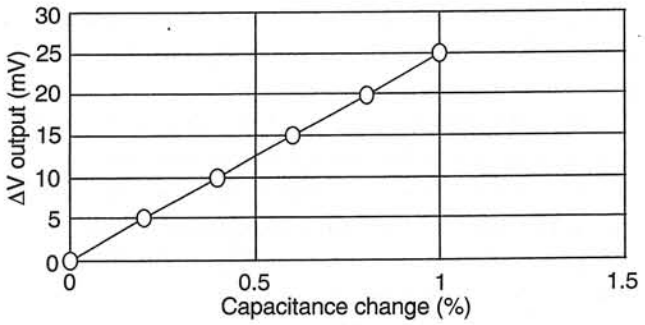

Fig. 3. Output voltage vs. capacitance change.

change is as large as 25 mV, which is large enough to be input into commercially available operational amplifiers. Good linearity is obtained in their relationship as shown in Fig. 3.

3. Ferroelectric thin film

3.1. Selection of bolometer material (BST vs. La modified SBN) and film preparation method

In order to develop a dielectric bolometer mode infrared detector, many ferroelectric materials, such as BST, SBN, PMN, and PST etc. [10], should be examined with the aim to get a strong dielectric--temperature dependence within the ambient temperature region, keeping a low leakage when operated. It is desired that lead-free materials are preferable for the Si-monolithic device as lead is easily soluble in SiO_2 film and fatigue induced by polarization reversal is bad. So, BST and SBN are studied for the candidate material of the bolometer.

Ferroelectric BST with perovskite structure possesses large temperature coefficient of dielectric constant around their Curie temperature (Tc) and Tc can be continuously modulated from 0°C to 70°C by controlling the Ba/Sr ratio. In addition, it exhibits characteristic features of diffuse phase transition, i.e., the ferroelectric phase transition takes place in a relatively wide temperature range near Tc with a very high-and-sharp dielectric peak. The high value in dielectric constant is essentially important in small element (say 50-μm square) of highly integrated pyroelectric array sensors to suppress switching noise by good capacitance match to the preamplifiers. On the other hand, ferroelectric $Sr_{0.5}Ba_{0.5}Nb_2O_6$ also possesses a large dielectric peak around Tc which can be continuously shifted from around 120°C down to room temperature by La^{3+} doping [11]. For lowering Tc, both substituting with La ($Sr_{0.48}Ba_{0.51}La_{0.01}Nb_2O_6$:SBLN) and excessive doping of La^{3+} ($Sr_{0.5}Ba_{0.5}Nb_2O_6$:2%La_2O_3:SBNL) are able to be employed. Figure 4(a) shows the temperature dependence of dielectric constant for the SBLN film. The dielectric constant increases gradually from 25°C with a drastic part in the range of 35°C to 50°C. The average temperature change rate of relative dielectric constant in the range is about 60/K or about 9%/K. It should be noted from Fig. 4(a) that the dielectric constant little changes around room temperature, which means in turn Tc for the SBLN is still higher, although the constant at over 40°C is fairly large as 60/K. This leads us to choose the BST for use in the dielectric bolometer detector rather than SBLN at this present stage.

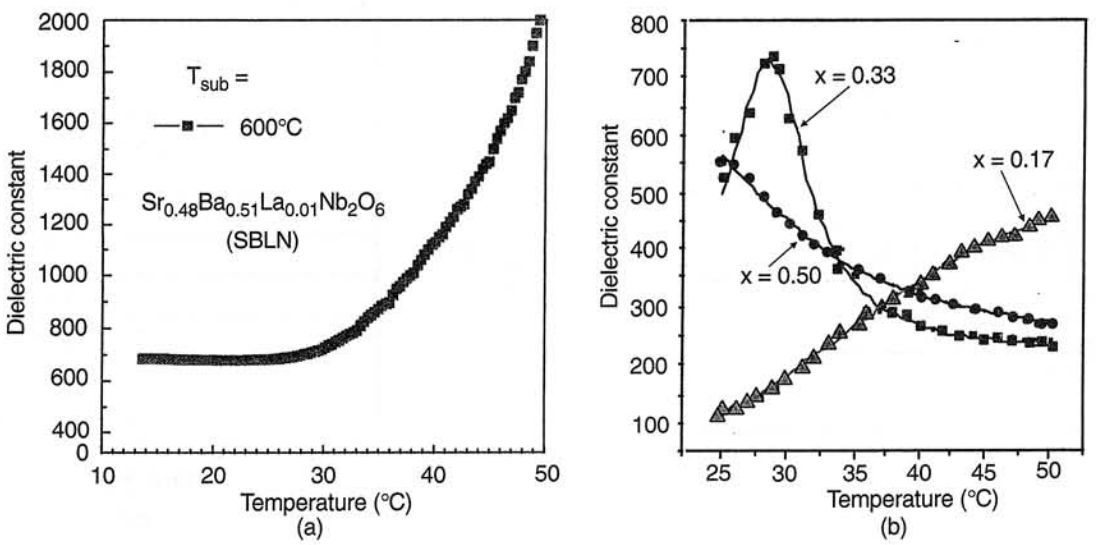

Fig. 4. Dielectric constant vs. temperature of $Sr_{0.48}Ba_{0.51}La_{0.01}Nb_2O_6$(SBLN) thin films deposited at Ts = 600°C (a), and dielectric constant vs. temperature of BST thin films of x = 0.17, 0.33 and 0.5 deposited at Ts = 500°C and 0.1 Torr (b).

It is required to develop ferroelectric thin film for use in the dielectric bolometer, where a large dε/dT is required at room temperature. BST films were fabricated by PLD method. Because evaporated particles from a BST target by strong laser beam are highly excited and the thin films can be prepared at low temperature, which is necessary not to damage the Si substrate having IC components. Crack-free and highly oriented films were successfully prepared on the Pt/Ti/SiO_2/Si(100) substrates in different ambient. The crystallinity of these films was examined by XRD analysis. Electrical properties such as leakage current, ferroelectric hysteresis loops, and temperature dependence of capacitance were also characterized.

3.2. Dielectric characteristics of BST films for dielectric bolometer mode capacitor

The BST films were deposited on Pt/Ti/SiO_2/Si(100) substrates above 450°C in O_2 gas of pressure about 13 Pa. N_2O gas instead of O_2 gas improved the crystallinity of BST thin films because of highly chemical activity due to oxygen atomic radicals produced by ultraviolet irradiation of ArF laser. X-ray diffraction pattern of the film has large peaks of (100), (110), and (112) planes. Temperature dependence of relative dielectric constant of the BST films shows a sharp change having a peak around room temperature, as shown in Fig. 4(b). A peak exists below 25°C in the film of Ba/Sr = 1 (x = 0.5), and shifts to above 50°C in the film of Ba/Sr = 6 (x = 0.17). For Ba/Sr = 2 (x = 0.33), the peak exists near 27°C and is very sharp. The differential relative dielectric constant against temperature is the largest for Ba/Sr = 2 among them and is about 100/K which is corresponding to 10%/K, where the absolute capacitance is about 640 pF at the pixel capacitor size of about 280 μm square. This value is equivalent to a pyroelectric coefficient of 1.8×10^{-7} C/cm^{2}K in the film of thickness 0.5 μm, capacitance area 8×10^{-4} cm^2, and bias field 20 kV/cm, which is almost the same as that of $LiTaO_3$ crystal. Relative dielectric constant of the BST film, which is about 450 at 25°C, changes by about 1 to 10%/K in room temperature. The maximum change in the relative dielectric constant is as large as about 100/K, and more than about 10%/K relative change in the dielectric constant has been obtained.

4. Membrane structure with high-temperature increment

4.1. Membrane structure of detector pixel

It is necessary to develop thermally insulated structure for the detector pixel by using simple Si-micromachining process with high reliability in thermal type of infrared sensors. The structure of sensing area usually requires a suspended membrane or bridge structure in order to improve their thermal isolation and obtain a large temperature rise in the detector pixel under IR irradiation. A cross-sectional view of our detector pixel part is shown in Fig. 5. After fabricating MOSFET circuit arrays, Si(110) wafer was preferentially etched from the backside by tetramethyl ammonium hidroxide (TMAH) and the membrane structure with the vertical sidewall was fabricated. Then the electrodes and ferroelectric thin film were deposited at low temperature.

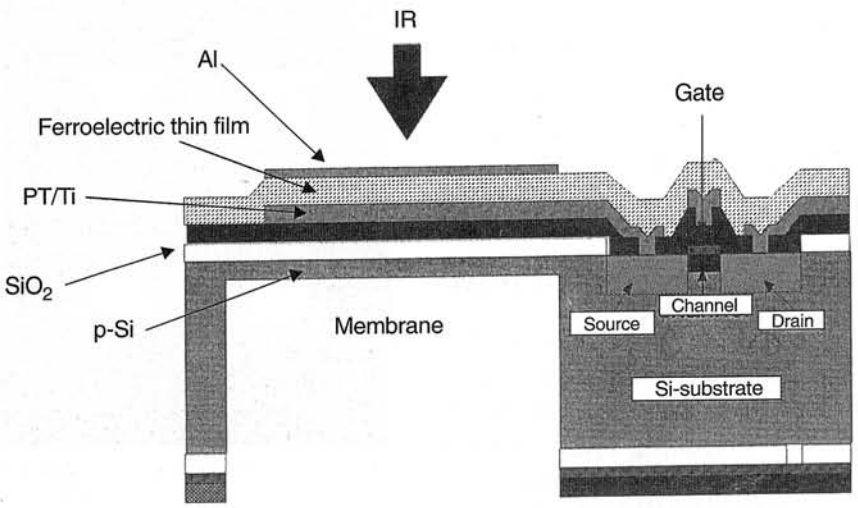

Fig. 5. A cross-sectional illustration of the detector pixel part.

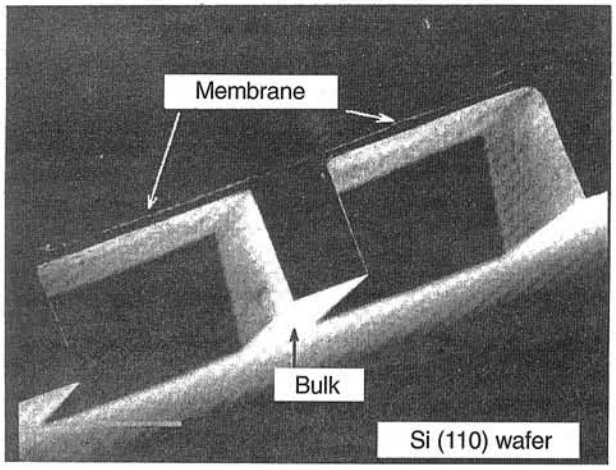

(a) Cross section

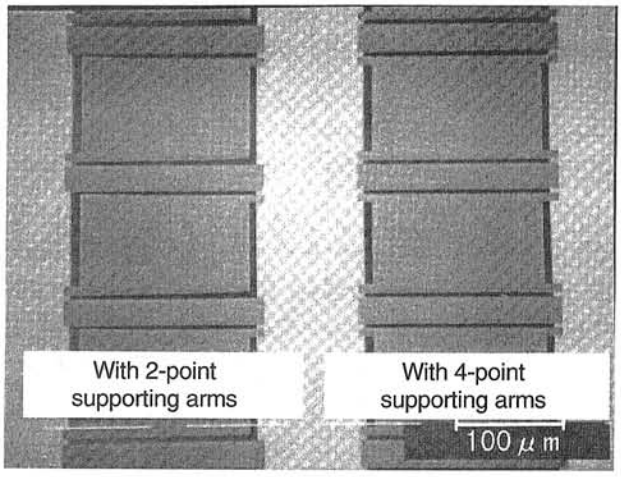

(b) Surface

Fig. 6. SEM photographs of the micro-structure in sensing area: cross section (a) and surface (b).

Figure 6(a) shows a cross-sectional view of the sensing area, etched for 3 hours at 90°C with TMAH (22 wt%) etchant. A high aspect ratio was achieved in etched shape using Si(110) wafer. Figure 6(b) shows an SEM photograph of surface area with 2-point-supporting arms and 4-point-supporting arms, respectively. The precise patterns without deformation by strain can be manufactured by the Si bulk-micromachining technology.

4.2. Temperature change in detector pixel

It is important to simulate the temperature increase in sensing area in order to evaluate the magnitude of output signal and design the signal processing circuit. The temperature increase in sensing area of several kinds of structures and materials was simulated by using thermal analysis simulator "ANSYS", which is a 3-dimensional thermal solver based on a finite element method. Linear and nonlinear analyses are available for steady-state and transient heat transfer with capabilities including conduction, convection, and radiation. One of the simulated temperature distribution on the membrane is shown in Fig. 7. The whole area of the sensor is irradiated homogeneously. In this figure, the pattern is a Si membrane with 4-point-supporting arms. Irradiated IR light density is assumed to be 500 μWcm^{-2}. Thermal energy diffuses into Si substrate through supporting arms of the membrane. Therefore, it is effective to enhance temperature increase:

- by using membrane materials with a small thermal conductivity, which is smaller for SiO_2 than for Si,
- by reducing the number of short and wide suspensions.

Optimum microstructures based on the thermal simulation were fabricated by Si anisotropic etching, as shown in Figs. 6(a) and (b).

A temperature increase in a detector pixel whose membrane is a Si etched layer as thin as about 50 μm by He-Ne laser illumination (388 $mWcm^{-2}$) to its surface was measured as shown in Fig. 8 by a "thermo-micro (6T04S)", which is a high-sensitive infrared microscopic thermometer using quantum cooling-type InSb detector, where minimum detective temperature difference is 1°C and spatial resolution is 10 μm. As is predicted by the above mentioned, it is clear that the increase in temperature is larger with 2-point supporting arms than with 4-point ones. A temperature increase of about 1.4°C was observed in the sensing

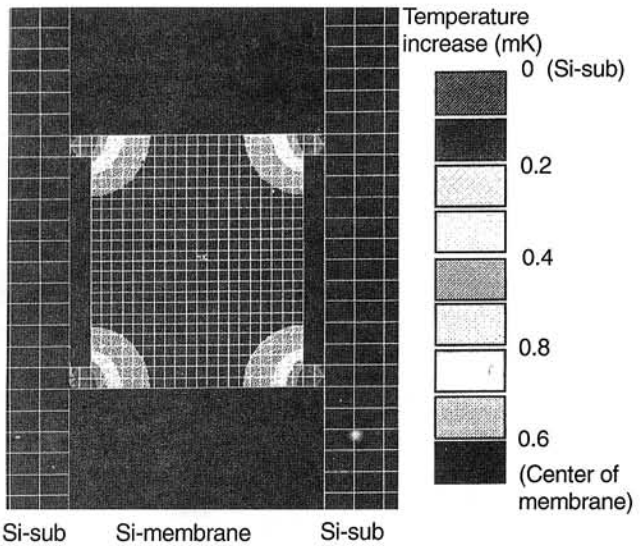

Fig. 7. Simulated temperature distribution on the floating membrane (material of membrane : Si, atmosphere: in air).

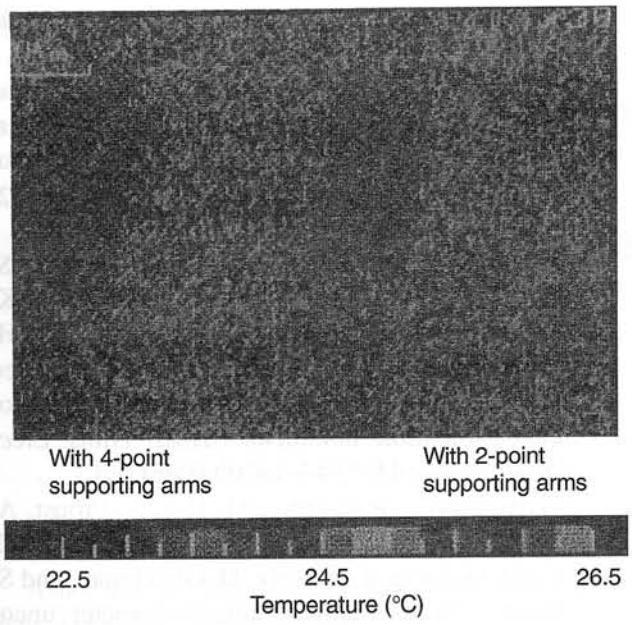

Fig. 8. Measured temperature distribution on the floating membranes with 4- and 2 points-supporting arms (material of membrane: Si, atmosphere: in air).

area with the 2-point-suspensions, which was consistent with our mentioned thermal simulation results.

5. Experimental results of infrared response in dielectric bolometer mode of detector pixel

The detector pixel and some resultant pixel arrays have been developed by combining both the MOSFET process and the micromachining process. Thereafter, the pixel arrays and their control circuits can be monolithically integrated. The fabricated membrane consists of Al/BST(1 μm)/ Pt(500 nm)/ SiO_2(1 μm)/Si multilayer, shows size of 500 μm square, and is supported by 2 beams. Figure 9 shows the output voltage (Vout) waveform in the detector pixel circuit fabricated as mentioned above. Applied pulse voltages are +1V and –1V. On-board evaluation has been carried out in the assembled circuit with a source-follower output, and it is found that the output level is about 40 mV when a relative capacitance change of the pixel is about 3%. It is considered that the circuit has enough output signal level for input of conventional operational amplifier. The relationship between the output voltage and capacitance change in the BST film in the assembled circuit agrees well with that in the corresponded simulation results.

We are afraid that the developed pixel cannot absorb infrared lays well enough because the top Al

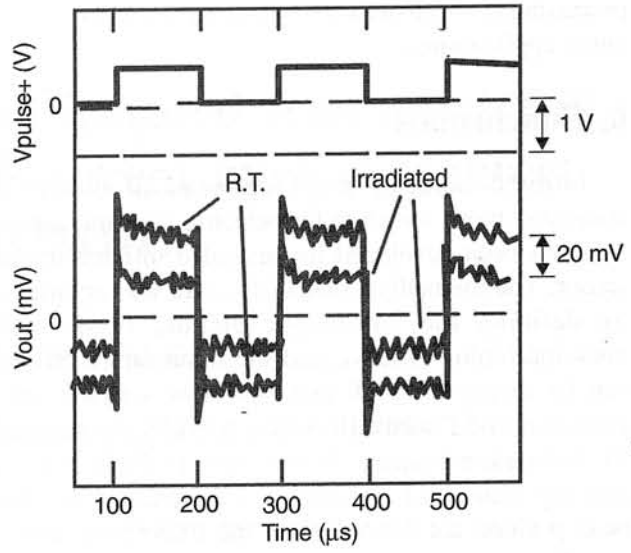

Fig. 9. Output voltage waveform in the detector pixel circuit with a source-follower output.

electrode should reflect major incident infrared lays. In our fabricated device, however, the surface of the Al electrode is found to be not so flat but fairly rough. This is because the BST film prepared by PLD method under the Al electrode has not a smooth surface. This leads the Al electrode to absorb a part of incident infrared lays. And infrared lays are detected in the experiment, even though the irradiation power density on the detector is very high (about 80 mW/cm^2). A new infrared absorbing layer is now planning to be formed on the upper electrode.

The experimental output of 40 mV per 3% change in the detecting BST capacitor seems to be low in comparison with the simulated result. This is unclear at present stage but one reason to note is that a source-follower output buffer was externally added to the output of the detector. And that the output level is found to be degraded by about 10% in the PSPICE simulation.

Finally, we have estimated sensor characteristics such as thermal responsivity R_v, and specific detectivity D^*. The temperature increase is simulated to be 10 mK for incident IR light density of 500 μW/cm^2 from thermal analysis of our thermally isolated diaphragm structure. Then R_v is calculated to be 50 kV/W at sensor electrode size of 100 μm square. Also D^* is expected to be 6.5×10^9 cmHz$^{1/2}$W^{-1}, as thermal noise V_n is assumed to be 770 nV for thermal noise of resistor and tan δ noise [12]. Especially, it is noted that the calculated D^* is fairly larger than those reported as the other type of IR sensors. This indicates that an IR sensor in dielectric bolometer mode based on ferroelectric thin film capacitors is expected to be

promising for high-sensitivity and high-resolution oriented applications.

6. Conclusions

Infrared detector pixel operated in dielectric bolometer mode based on ferroelectric thin film capacitors has been developed for uncooled infrared image sensor. The thermally isolated structure was optimized by defining the anisotropic etching in Si bulk micromachining process, and the temperature change can be increased. BST thin film was selected after comparing BST with SBLN as a ferroelectric material for dielectric bolometer, and prepared by PLD method, and the change of dielectric constant and dielectric peak position are dependent on the Ba/Sr ratio, corresponding to ferroelectric thin film characteristics. The maximum temperature coefficient of dielectric constant is as large as 10%/K. The proposed circuit, capacitor-capacitor serially connected circuit, where at least one capacitor is composed of a BST ferroelectric thin film was evaluated by PSPICE simulation. When a relative capacitance change in the BST ferroelectric capacitor of the detector circuit is 1%, the output level was about 25 mV. The above circuit on-board with a BST thin film capacitor on a Si membrane structure was assembled and it is confirmed that the relationship between the output level and capacitance change in the BST thin film in the assembled circuit agrees well with that in the corresponded simulation results. Calculated thermal responsivity R_v is 50 kV/W, expected detectivity D^* is 6.5×10^9 $cmHz^{1/2}W^{-1}$, and higher-sensitivity is anticipated in comparison with the other type of IR sensors.

Acknowledgments

The authors would like to thank all members of SEIS Group and all fellow researchers in Okuyama Lab. in Osaka University for their valuable advice and help. The technical support of Technology Research Institute of Osaka prefecture for this work is greatly appreciated. The financial support of Osaka prefecture is also appreciated.

References

1. C. Hanson, H. Beratan, R. Owen, M. Corbin, and S. Mckenny, "Uncooled thermal imaging at Texas Instruments", *Proc. SPIE* **1735**, 17–26 (1992).
2. R. Watton, "Ferroelectric materials and IR bolometer arrays: from hybrid arrays towards integration", *Integrated Ferroelectrics* **4**, 175–186 (1994).
3. M. Ueno, O. Kaneda, T. Ishikawa, K. Yamada, A. Yamada, M. Kimata and M. Nunoshita, "Monolithic uncooled infrared image sensor with 160×120 pixels", *Proc. SPIE* **2552**, 636–643 (1995).
4. A. Tanaka, S. Matsumoto, N. Tsukamoto, S. Itoh, K. Chiba, T. Endoh, A. Nakazato, K. Okuyama, Y. Kumazawa, M. Hijikawa, H. Gotoh, T. Tanaka, and N. Teranishi, "Infrared focal plane array incorporating silicon IC process compatible bolometer", *IEEE Trans. Electron Devices* **43**, 1844–1850 (1996).
5. W. Radford, D. Murphy, M. Ray, S. Propst, A. Kenndy, J. Kojiro, J. Woolaway, K. Soch, R. Coda, G. Lung, E. Moody, D. Gleichman, and S. Baur, "320×240 silicon microbolometer uncooled IRFPAs with on-chip offset correction", *Proc. SPIE* **2746**, 82–92 (1996).
6. R. Owen, J. Belcher, H. Beratan, and S. Frank, "Producibility advances in hybrid uncooled infrared devices – II", *Proc. SPIE* **2746**, 101–112 (1996).
7. Y. Takada, M. Ikari, S. Kirihara, K. Uchizawa, and R. Taniguchi, "Microminiature PIR human body detecting sensor", *Proc. Tech. Dig. 16th Sensor Sym.*, 231–234 (1998).
8. K. Hashimoto, M. Noda, R. Kubo, T. Mukaigawa, H. Tanaka, H. Xu, and M. Okuyama, "Detector pixel in dielectric bolometer mode based on ferroelectric thin film capacitors for uncooled infrared image sensor", *Proc. Technical Dig. 16th Sensor Symp.*, 69–72 (1998).
9. M. Noda, R. Kubo, H. Tanaka, T. Mukaigawa, K. Hashimoto, H. Xu, and M. Okuyama, "A new type of dielectric bolometer mode of detector pixel using ferroelectric thin film capacitors for infrared image sensor", *Proc. SPIE* **3436**, 660–667 (1998).
10. D.E. Witter, H.R. Beratan, B.M. Kulwicki, and A. Amin, "Pyroelectric materials for uncooled IR detectors", *Infrared Technology*, 19–26 (1994).
11. S.T. Liu and R.B. Maciolek, "Rare-earth-modified $Sr_{0.5}Ba_{0.5}Nb_2O_6$ ferroelectric crystals and their application as infrared detectors", *J. Electron. Mat.* **4**, 91–100 (1975).
12. C.M. Hanson, "Hybrid pyroelectric-ferroelectric bolometer arrays", in *Semiconductors and Semimetals,* vol. 47, pp. 123–174, edited by P.W. Kruse and D.D. Skatrud, Academic Press, San Diego, 1997.

